THE JOURNAL OF PHYSICAL CHEMISTRY B

Article

pubs.acs.org/JPCB

Polymer Binding to Carbon Nanotubes in Aqueous Dispersions: Residence Time on the Nanotube Surface As Obtained by NMR Diffusometry

Anton E. Frise,[†] Guilhem Pagès,[†,‡] Michael Shtein,[§] Ilan Pri Bar,[§] Oren Regev,[§,∥] and István Furó*[,†]

[†]Division of Applied Physical Chemistry and Industrial NMR Centre, Department of Chemistry, Teknikringen 30-36, KTH Royal Institute of Technology, SE-10044 Stockholm, Sweden

[‡]Wallenberg Wood Science Centre (WWSC), Teknikringen 56-58, KTH Royal Institute of Technology, SE-10044 Stockholm, Sweden

[§]Department of Chemical Engineering and [∥]The Ilse Katz Institute for Meso and Nanoscale Science and Technology, Ben-Gurion University of the Negev, 84105 Beer-Sheva, Israel

ABSTRACT: The binding of block copolymer Pluronic F-127 in aqueous dispersions of single- (SWCNT) and multiwalled (MWCNT) carbon nanotubes has been studied by pulsed-field-gradient (PFG) ^{1}H NMR spectroscopy. We show that a major fraction of polymers exist as a free species while a minor fraction is bound to the carbon nanotubes (CNT). The polymers exchange between these two states with residence times on the nanotube surface of 24 ± 5 ms for SWCNT and of 54 ± 11 ms for MWCNT. The CNT concentration in the solution was determined by improved thermal gravimetric analysis (TGA) indicating that the concentration of SWCNT dispersed by F-127 was significantly higher than that for MWCNT. For SWCNT, the area per adsorbed Pluronic F-127 molecule is estimated to be about 40 nm^2.

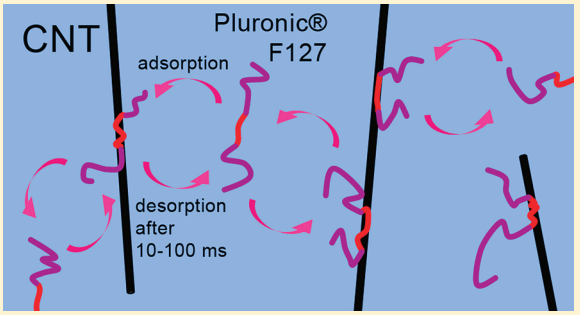

INTRODUCTION

Carbon nanotubes (CNT) have unique electronic, chemical, and mechanical properties[1] and are therefore of interest for application in molecular electronics,[2,3] sensors,[4] and in drug delivery.[5] CNT tend to bundle into strongly bound aggregates due to van der Waals forces, and the formation of such aggregates impedes their implementation.[6] Therefore, debundling of the CNT aggregates is required by exfoliating and dispersing CNT. One approach to facilitate CNT dispersion is the chemical modification of their surface by covalent binding of molecules.[7] This, however, changes the molecular structure of the CNT and might therefore affect their properties. Alternatively, addition of various types of dispersant molecules (surfactants, polymers, or biomolecules) that physically adsorb to the CNT surface may prove effective, while simultaneously preserving the molecular structure of the CNT.[8] Long and linear polymers such as polyvinyl pyrrolidone (PVP) and polystyrene sulfonate (PSS) have been reported to wrap tightly around the CNT via specific molecular interations.[9−11] Although effective in dispersing the CNT by screening of their hydrophobic surface from water, such formation of strongly associated composites may also alter the electronic properties of both polymer and CNT components.[9,12] On the other hand, block-copolymers such as poloxamers (Pluronics) consisting of hydrophobic and hydrophilic moieties provide a softer route toward the dispersion of CNT. Indeed, the use of Pluronics for dispersing CNT has attracted a lot of interest.[9,13−18] Here, the hydrophobic part is believed to be attached at the CNT/water interface by a "non-wrapping" interaction, whereas the hydrophilic parts are extended out into the aqueous phase, providing a steric barrier and preventing CNT reaggregation.[9,16] For optimization of CNT dispersion by physical adsorption it is important to obtain a detailed understanding of dispersant/CNT binding mechanism: What dispersant concentration is required? How much of the dispersant is on the CNT surface and how long do individual molecules stay there? What is the nature of dispersant structures and distribution on the CNT surface?

The aim of this paper is to investigate some of these questions. Previously, we showed that the diffusion behavior of bovine serum albumin (BSA) in dispersions of CNT, obtained by pulsed-field-gradient (PFG) NMR, could provide information on the fractions of proteins bound to the CNT as well as establish that the BSA molecules exchange rapidly (≪50 ms) between bound and free states on the experimental time scale.[19] Previously, the adsorption of surfactant Tween80 on SWCNT was also investigated by PFG-NMR[20] and there the exchange was concluded to be slow (≫100 ms) on the same experimental time scale. However, in none of those cases was any information gained on the actual value of the residence time on the CNT surface and its sensitivity to system parameters such as dispersant

Received: October 12, 2011
Revised: January 31, 2012
Published: January 31, 2012

   dx.doi.org/10.1021/jp209800u | *J. Phys. Chem. B* 2012, 116, 2635−2642

type or CNT surface energy. Herein, we present a PFG-NMR study of the diffusion behavior of block copolymer Pluronics F-127 (see Figure 1) in dispersions of SWCNT and MWCNT.

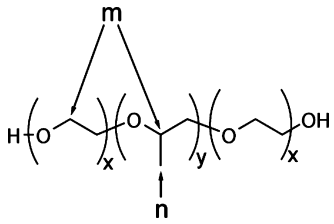

Figure 1. Molecular structure of Pluronics F-127, with x = 97 and y = 69 and molecular weight of 12 600. Methylene protons denoted by "m" provide one peak while methyl groups, denoted by "n", in the PPO blocks provide another peak in the ^{1}H NMR spectrum.

The exchange process of polymers between free and bound states has been carefully investigated by observing diffusional signal decays for different diffusion times varied in the range 10 - 500 ms. These times were longer (by many orders of magnitude) than the time scales in investigations of similar polymer/CNT dispersions by electron paramagnetic resonance (EPR)[15] or by computer simulations of the molecular dynamics (MD).[14,16,21−30] As we show below, PFG-NMR is capable to provide unique and complementary information on the time regime for dispersant exchange between bound and free states.

EXPERIMENTAL SECTION

Materials. SWCNT (outer diameter = 1.2−1.5 nm, length = 2−5 μm, BET surface area = 283 m^2/g, produced by the electric arc discharge method, Carbolex AP-grade) and Pluronic F-127 (with approximate molecular mass of 12500) were purchased from Sigma-Aldrich Co. MWCNT (outer diameter = 10−20 nm, length = 1−5 μm, produced by chemical vapor deposition method, PD15L1−5-COOH, batch 111909) partially surface functionalized with 2.1 atom % COOH groups were purchased from NanoLab, Inc. Heavy water (99.9 atom % D) was purchased from Isotec, Inc. All materials were used as received.

Thermal Gravimetric Analysis (TGA). Two solutions of SWCNT and MWCNT (solution 1 and 2, respectively, see Table 1 for initially added amounts) were prepared by bath sonication in an Elmasonic S 10 (30 W, 37 kHz). The water level and temperature in the bath were kept constant and the vial (charged with 10 mL solution in distillated water) was placed in the center of the bath. The postsonication dispersions were then centrifuged (Heraeus Megafuge 1.0) for 20 min at 4000 g. Following sonication and centrifugation, a phase separation of supernatant and precipitate was performed by decantation. The supernatants were visually clear (however black in the case of the SWCNT dispersion and only dark gray in the case of the MWCNT dispersion, vide infra). The supernatant was lyophilized for 48 h. The precipitate was filtered on a cellulose acetate/cellulose nitrate MF-Millipore membrane filter (0.22 μm pore size) placed on a vacuumed sintered glass funnel, washed with 30−40 mL distillated water and dried for 16 h in vacuum at 100 °C. The weights of the dried sample portions, supernatant and precipitate, were measured on an analytical balance accurate to 0.01 mg. The relative amount of F-127 left in each fraction was analyzed by a TGA-Mettler Toledo Star System (Mettler TGA/STDA85) under N_2 at a flow rate of 200 mL/min at a heating rate of 10 °C/min from 30 to 430 °C (well above the dispersants boiling or decomposition point) using aluminum crucibles of 100 μL volume. TGA of pure F-127 indicated its total decomposition under these TGA conditions (Insert in Figure 2). The concentration of the CNT in the supernatant can be calculated in two independent ways, either via eq 1 or via eq 2:

$$[\mathrm{CNT}]_s = \{M_s(1 - \varphi_s)\}/V_s \quad (1)$$

$$[\mathrm{CNT}]_s = \{M_{\mathrm{CNT}} - M_p(1 - \varphi_p)\}/V_s \quad (2)$$

where $[\mathrm{CNT}]_s$ is the CNT mass concentration in the supernatant, V_s is the volume of supernatant, M_x the weight of dried CNT/F-127 portions, and φ_x is the weight fraction of F-127 within a given dried portion as determined by TGA, with subscript "x" being either "s" or "p" indicating supernatant and precipitate, respectively. M_{CNT} is the total mass of CNT originally weighed in a sample. Table 1 summarizes the nominal initial and actual (as calculated from TGA) component masses in the supernatant. The derived concentrations are presented in Table 2.

Table 1. Weights of CNT and F-127 Initially Added into Solutions 1 and 2, and F-127 Mass Fractions (φ) in the Precipitate and Supernatant, As Calculated from TGA Results (Table 2)

	solution 1/SWCNT		solution 2/MWCNT	
	mass (mg)		mass (mg)	
initial CNT mass (M_{CNT})	31.46		27.41	
initial F-127 mass	31.26		28.73	
total initial mass	62.72		56.14	
		φ		φ
dried supernatant mass (M_s)	58.62	0.48	33.02	0.65
dried precipitate mass (M_p)	1.50	ND[a]	19.83	0.20
total weight work up (M_s + M_p)	60.12		52.85	

[a]Not determined; the small quantity of the precipitate does not allow accurate TGA analysis.

Diffusional Behavior Observed by NMR Spectroscopy. Aqueous dispersions of CNT for the diffusion measurements were prepared with concentrations given in Table 2. In a reference solution (solution R), only the F-127 polymer was dissolved in heavy water (D_2O). SWCNT or MWCNT were added to solution R to yield solutions 3 and 4, respectively. The CNT in solutions 3 and 4 were dispersed by bath sonication in a Branson 2200 Ultrasonic (60 W, 47 kHz). The temperature was kept at ca. 20 °C by leading a steady flow of tap water through the water bath. Solutions 3 and 4 were then centrifuged (Wifug) for 25 min at 6200 g until the supernatants became visually clear, after which they were collected. All solutions were stored in a fridge at 4 °C until further use.

The NMR measurements were performed on a Bruker 300 Avance III spectrometer (7.0 T) operating at 300.09 MHz for proton (^{1}H), equipped with a DIFF-25 Bruker diffusion probe. The probe has the capacity for generating magnetic field gradient pulses with a maximum gradient value of 9.7 T/m. The gradient strength was calibrated by measuring water diffusion (1.90×10^{-9} m^2/s for residual HDO in a D_2O solution at 25 °C[31]). The temperature at the sample position was confirmed with an external thermocouple. Prior to the NMR diffusion measurements the longitudinal (T_1) and transverse (T_2) relaxation times were measured by conventional inversion−recovery and spin−echo experiments, respectively. All relaxation decays were, within

dx.doi.org/10.1021/jp209800u | J. Phys. Chem. B 2012, 116, 2635−2642

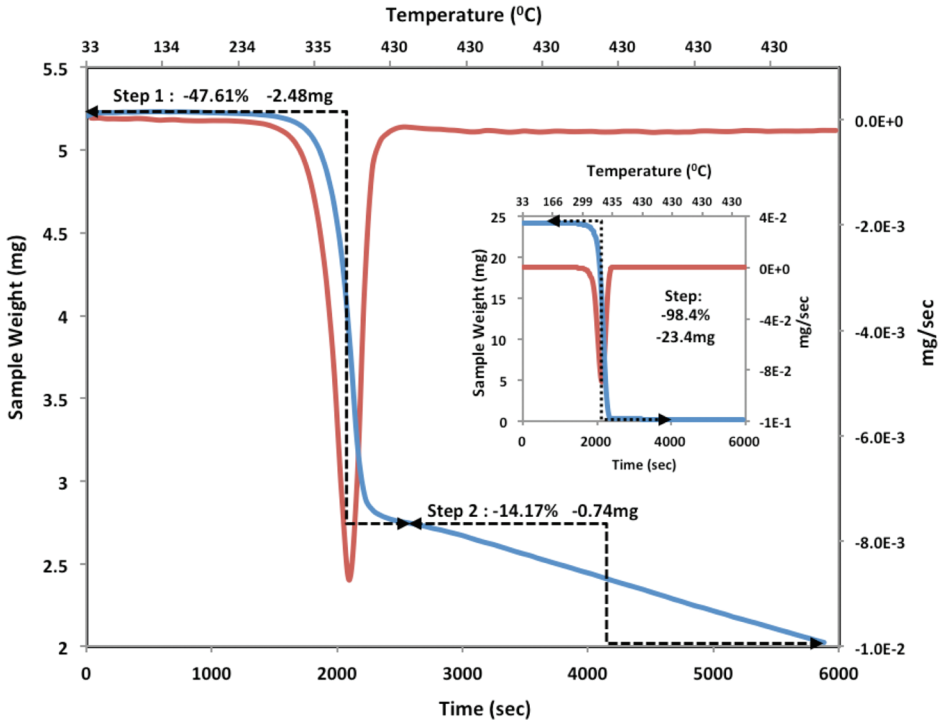

Figure 2. Thermogram of the dried supernatant of solution 1. Inset: thermogram of pure F-127. The blue curve indicates the sample weight (mg) with respect to time (s) and temperature (°C, note the double *x* axis). The red curve is the time derivative of the sample weight (mg/s). The weight-loss at ca. 385 °C corresponds to decomposition of F-127.

Table 2. Supernatant Concentrations (mg/mL) for Components in the Investigated Solutions, As Derived from the Initial Weights and As Determined by Either TGA or NMR

	TGA				NMR			
	solution 1		solution 2		solution 3[d]		solution 4[d]	
	initial	determined	initial	determined	initial	determined	initial	determined
F-127	3.13	2.81	2.87	2.15[c]	3.32	ND[a]	3.32	2.79
SWCNT	3.15	3.05			3.31	ND[b]		
MWCNT			2.74	1.16			3.33	ND[b]

[a]Overlap of HDO and F-127 spectral peaks prohibited accurate estimation of the polymer concentration. [b]The CNT do not exhibit peaks in the ^{1}H NMR spectra. [c]The difference between initial and determined masses is caused by F-127 depletion to the precipitate. [d]The F-127 concentration in solution R is the same as in solutions 3 and 4.

the experimental error, single-exponential. For all Pluronics peaks the T_1 relaxation times were slightly below 500 ms and the recycle delays were set to 2.6 s (>5 × T_1). The 90° excitation pulse length was ~10 μs.

Diffusion measurements were performed with the stimulated echo pulse sequence. Gradient pulse lengths (δ) were set to 2 ms and gradient recovery times to 1 ms. Different diffusion times (Δ) were set as described in the Results and Discussion. In each experiment the gradient pulse strength (g) was increased stepwise, with the number of gradient steps between 16 and 48 and the number of scans for each gradient step between 16 and 256. The value of maximum gradient, the numbers of steps and scans per step were chosen to obtain signal decays of at least 3 orders of magnitude for solutions *R* and 4, while simultaneously avoiding gradient strengths higher than 80% of the max gradient (i.e., 7.8 T/m). The signal decays for solution 3 were limited by long experimental times to one or 2 orders of magnitude. This was the result of a low signal-to-noise ratio due to fast transverse relaxation in this sample (see the Results and Discussion). The micellization of F-127 above certain concentrations and temperatures has been observed in a previous study.[32] Formation of micelles introduces another diffusing state for the polymers, with a diffusion rate that is expected to be in between that of free and CNT-bound polymers. In such case, it would become more difficult to perform a detailed investigation of the polymer association to CNT. Thus, all diffusion measurements were performed on samples of sufficiently low concentration (yet, still above what is needed for dispersing the CNT[13,14,16]) and always at 20 °C where micelles are not formed.

RESULTS AND DISCUSSION

Redistribution of the Molecular Components in the Dispersion. The determination of the concentration of dispersed CNT in solution is a challenging task since both dispersant and CNT are distributed between the supernatant and precipitate phase.[33,34] The information of CNT concentration in solutions is of great importance in mechanistic studies but is essential when CNT are integrated in a polymer matrix and the properties of the final composite are dictated in most cases by the CNT concentration. Figure 2 shows a thermogram example for determining F-127 residue in the separated supernatant sample and calculating the mass of the polymer component in

dx.doi.org/10.1021/jp209800u | J. Phys. Chem. B 2012, 116, 2635−2642

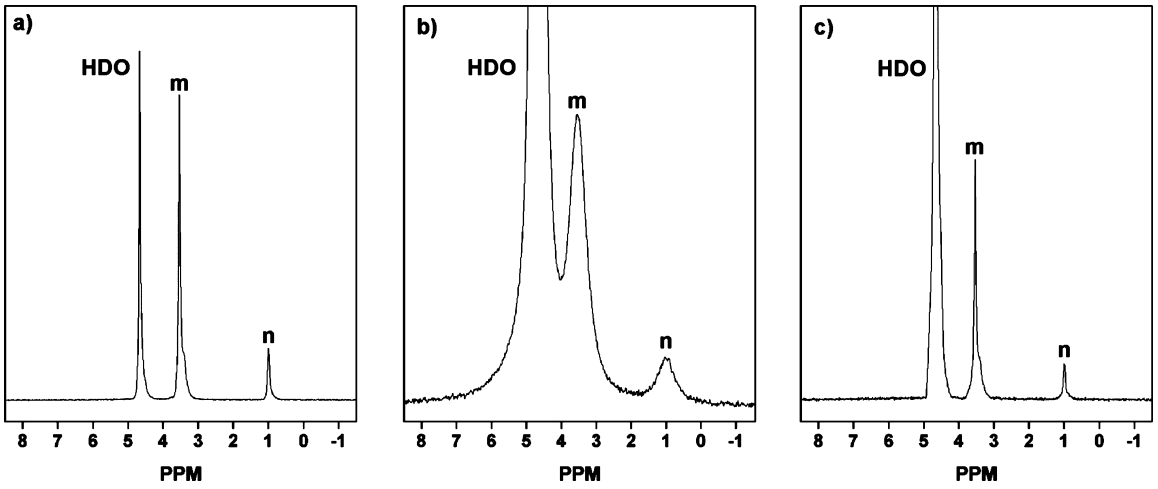

Figure 3. ^{1}H NMR spectra of Pluronics F-127 in (a) aqueous solution (solution *R*), (b) solution with SWCNT (solution 3), and (c) solution with MWCNT (solution 4). The signals from HDO, methylene (m) and methyl (n) protons are indicated. The HDO signal intensity with respect to the F-127 signals varies strongly, primarily because of different HDO relaxation times in the solutions.

the CNT/F-127 mixture obtained by drying the supernatant portion of the SWCNT dispersion. The concentrations of different components in solutions 1−4 are presented in Table 2.

The concentration of MWCNT in the supernatant was first calculated via eq 1 and the data in Table 1, and found to be 1.16 mg/mL. Alternatively, one can exploit eq 2 to calculate the concentration of the MWCNT in the supernatant as {27.41−19.83 × (1−0.20)}/10 = 1.15 mg/mL. The resulting calculated concentration is in perfect agreement with the previous calculation (based on eq 1) and validates the proposed TGA-based approach. Similarly, the concentration of SWCNT in the supernatant is calculated by eq 1 to be 3.07 mg/mL, which is much higher than the concentration of the MWCNT solution, in agreement with the ocular observation (see experimental).

The dispersion of MWCNT following sonication with F-127 as dispersant was analyzed with TGA by two independent measurements (direct analysis of the supernatant and by mass balance, through the determination of the amount of CNT in the precipitate). As shown above, the results of the two measurements match within ±1%. On the other hand, the mass loss during the analysis process is considerable and that may limit accuracy to the order of 5−10%. Irrespective of that, the data clearly indicate that F-127 disperses SWCNT much better than MWCNT, by a factor of ca. 2.7. The MWCNT consist of many concentric tubes where the intermediate surfaces are inaccessible to the F-127. Thus, the accessible specific surface area (SSA) of SWCNT (283 m^2/g) is expected to be higher than that of MWCNT. These two factors (larger amount of dispersed SWCNT and higher accessible SSA) imply that the CNT surface available for F-127 adsorption should be much larger in the SWCNT dispersion as compared to the MWCNT dispersion.

From the TGA measurements the supernatant concentrations of F-127 were found to be 2.81 mg/mL and 2.15 mg/mL for SWCNT and MWCNT supernatants, respectively (see Table 2). These concentrations are lower (by ca. 10% and 25%) than the initial amounts of F-127 due its depletion of from the supernatant by binding to the precipitate.

The F-127 concentration can also be estimated from the NMR signal intensities, in contrast to the CNT that do not provide ^{1}H NMR signal. The ^{1}H NMR spectra for solutions *R*, 3, and 4 are shown in Figure 3. The transverse relaxation times T_2 in solutions *R* and 4 were long (>100 ms) and the spectral peaks were well resolved (see Figures 3a and c). In solution 3, T_2 is reduced to ca. 5 ms by paramagnetic and presumably metallic particles residual from the synthesis of SWCNT.[35] The resulting spectrum was therefore broad, with significant overlap of the spectral peaks as can be seen in Figure 3b. (If any, paramagnetic particles originally present in the MWCNT material must have been eliminated by the refluxing in sulfuric/nitric acid.[36]) Hence, in solutions *R* and 4 it was straightforward to compare the spectra, which yielded that the integral intensity of F-127 peaks in solution 4 was about 16% lower than that in solution *R*. The simplest explanation for this is the depletion of F-127 to the precipitate as has also been detected by TGA; the numbers (16% by NMR and 25% by TGA) are roughly consistent. We note that strong binding with long (>s or longer) residence times of F-127 to the CNT could, by very large broadening of the ^{1}H signal, also lead to an intensity loss. In the light of the diffusion results below this scenario is deemed to be improbable.

NMR Diffusion and Polymer Exchange between Free and Bound States. As illustrated in Figure 4, the diffusional

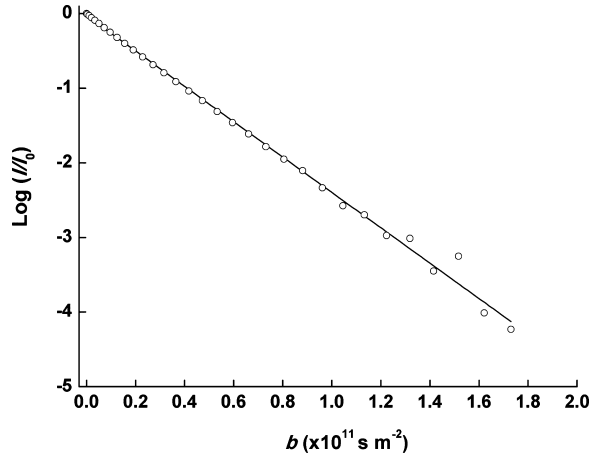

Figure 4. Diffusional decay on base-10 logarithmic scale of the NMR signal intensity of the methylene protons (m) of Pluronics F-127 (3.32 mg/mL, 0.3 wt %) in solution *R* and best fit of eq 3 (solid line). *b* is the Stejskal−Tanner[37] factor, $(\gamma g\delta)^2(\Delta - \delta/3)$. The obtained self-diffusion coefficient of free polymer chains is 5.7 × 10^{-11} m^2/s.

dx.doi.org/10.1021/jp209800u | J. Phys. Chem. B 2012, 116, 2635−2642

decay of the ^{1}H NMR signal of F-127 is single-exponential. This indicates that micellization is not significant and that polydispersity is not large. The diffusion coefficient of individual polymer chains was then obtained by fitting the well-known Stejskal–Tanner equation[37]

$$I/I_0 = \exp(-(\gamma g \delta)^2(\Delta - \delta/3)D) \quad (3)$$

to the signal intensities I normalized by the signal intensity without gradient, I_0; γ is the magnetogyric ratio of ^{1}H. The self-diffusion coefficient D for F-127 was obtained to 5.7×10^{-11} m^2/s, which is in good agreement with previous observations.[32]

In the diffusion measurement of solution 3, error from the overlap of F-127 and HDO peaks was avoided by choosing starting values of the gradient so that the peak of the quickly diffusing HDO molecules was suppressed. For both solutions 3 and 4, we found that, in contrast to the neat polymer solution, the diffusional decay of the signal is not single-exponential. This is clearly illustrated in Figure 5. Hence, the polymer must have

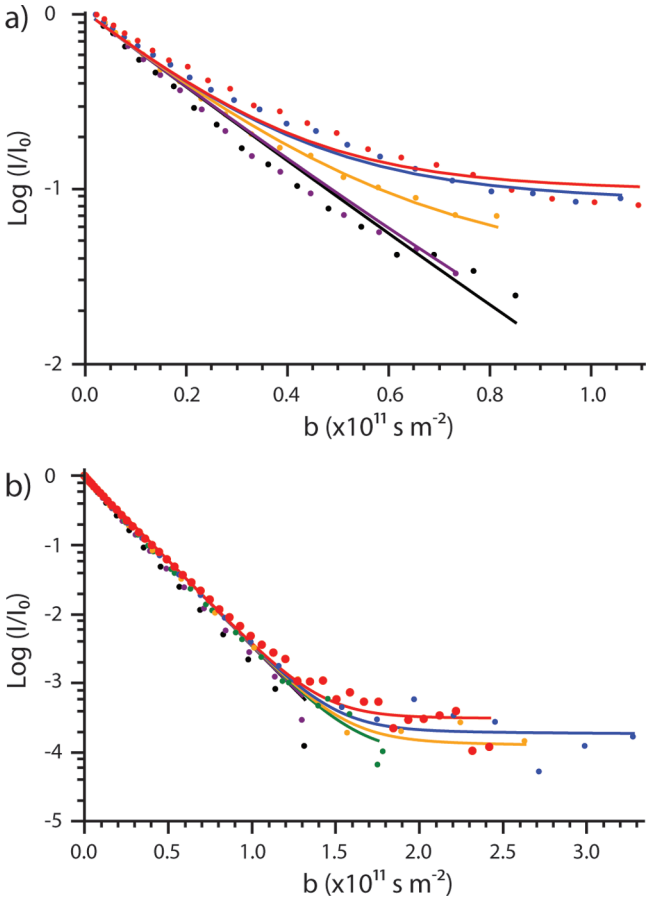

Figure 5. Diffusional signal decays on base-10 logarithmic scale and best fit of eqs 5 and 6 to all the data simultaneously. (a) Solution 3 with SWCNT (Δ = 10 (red), 20 (blue), 50 (yellow), 250 (purple), and 500 (black) ms) and (b) solution 4 with MWCNT (Δ = 20 (red), 50 (blue), 75 (yellow), 100 (green), 200 (purple), and 300 (black) ms). The fat dots in (b) provide an illustration of the significant deviation from single-exponential decay (see also Figure 4). b is as defined in Figure 4.

several different states in the CNT solution. Since the initial decay is similar to that exhibited by the neat polymer solution, we identify one state as free polymer chains in solution. The other state that leads to the component of the decay with a slower rate must arise from polymers that diffuse much slower. These polymers are identified as bound to CNT. The large size of the CNT ($\sim\mu$m in length) implies that they exhibit very slow (in the order or below $D \leq 10^{-14}$ m^2/s) Brownian motion, which thereby would result in negligible diffusional decay of the NMR signal of polymers attached to them.

The nonexponential diffusional decay indicates that the exchange of the polymer molecules between the two states, either bound to the CNT or free in the bulk solution, is not fast on the experimental time scale set by the diffusion time Δ. This is in contrast to what has been observed for the association of BSA to CNT.[19] On the other hand, the lack of fast exchange was also concluded for another nonionic surfactant Tween80 bound to SWCNT.[20] That dispersant is also characterized by having a polyethyleneoxide polar head. In contrast to that latter study,[20] here we can determine the actual residence times because, as can be seen in Figure 5, the character of the diffusional decay changes by varying the diffusion time Δ. Qualitatively, at diffusion times much shorter than the residence times of the polymer molecules in their different states the diffusional decay is the population-weighed sum of two distinct decays, each as in eq 3, with their respective characteristic diffusion coefficients, one that of the free polymers and one that of the CNT (we neglect here the possibility of the polymers diffusing along the CNT surface). In the opposite limit of fast exchange, the diffusion time is much longer than the residence times and the decay is single exponential with D being the population average of the two characteristic diffusion coefficients. As the diffusion time varies between these two limits, the diffusional decay changes character as is, indeed, observed in Figure 5.

Since the system is in equilibrium, there exists a detailed balance. Hence, the fractions of polymers in the free and bound states (p_{free} and p_{bound}, respectively) are related to the respective residence times in each state (τ_{free} and τ_{bound}) as

$$p_{free} = \frac{\tau_{free}}{\tau_{bound} + \tau_{free}} \quad (4a)$$

$$p_{bound} = \frac{\tau_{bound}}{\tau_{bound} + \tau_{free}} \quad (4b)$$

With this result at hand, the general expression for the diffusional decay at any diffusion time Δ becomes[38,39]

$$I/I_0 = p_1 \exp(-(\gamma g \delta)^2(\Delta - \delta/3)D_1) + p_2 \exp(-(\gamma g \delta)^2(\Delta - \delta/3)D_2) \quad (5)$$

where

$$D_{1,2} = \frac{1}{2}\left\{D_{free} + D_{bound} + \frac{1}{(\gamma g \delta)^2}\left(\frac{1}{\tau_{free}} + \frac{1}{\tau_{bound}}\right) \mp \left\{\left(D_{bound} - D_{free} + \frac{1}{(\gamma g \delta)^2}\left(\frac{1}{\tau_{bound}} - \frac{1}{\tau_{free}}\right)\right)^2 + \frac{4}{(\gamma g \delta)^4 \tau_{free}\tau_{bound}}\right\}^{1/2}\right\} \quad (6a)$$

and

$$p_1 = 1 - p_2 \quad (6b)$$

dx.doi.org/10.1021/jp209800u | J. Phys. Chem. B 2012, 116, 2635–2642

$$p_2 = \frac{1}{D_2 - D_1}(p_{\text{free}}D_{\text{free}} + p_{\text{bound}}D_{\text{bound}} - D_1) \quad (6c)$$

Note that different relaxation times, both for T_1 and T_2, in the bound and free states are not considered here (additional terms to account for such difference[40,41] can be included in eqs 5 and 6). In addition, in our system we only observed single component relaxations for all solutions.

Diffusion measurements were performed with Δ values between 10 and 500 ms for solution 3 with SWCNT and between 20 and 300 ms for solution 4 with MWCNT. In the analysis, the diffusion coefficient of free polymers was set to $D_{\text{free}} = 5.7 \times 10^{-11}$ m^2/s, equal to that obtained in solution *R* while the diffusion coefficients of F-127 in its bound state was set to $D_{\text{bound}} = 0$ (setting any value $<10^{-14}$ m^2/s makes no practical difference). With those parameters fixed, eqs 5 and 6 were simultaneously fitted with the two remaining free parameters τ_{bound} and τ_{free} to all collected diffusion decays in a particular solution. The fits are presented in Figure 5 and the obtained parameters are listed in Table 3.

Table 3. Residence Times (τ) and Calculated Fractions (p) for F-127 on Nanotube Surfaces and in Solution, in SWCNT and MWCNT Dispersions

	solution 3/SWCNT		solution 4/MWCNT	
	time (s)	2σ (s)	time (s)	2σ (s)
τ_{bound}	0.024	0.005	0.054	0.011
τ_{free}	0.155	0.042	126.7	42.8
	fraction (%)		fraction (%)	
p_{bound}	14		0.04	
p_{free}	86		99.96	

As seen in Figure 5, the scatter of data points around the fitted functions was quite large. Nevertheless, the deviation from single exponential decays is significant in both SWNT and MWNT dispersions. The scatter is due to low signal-to-noise ratios, especially at high gradient strength. Systematic deviations between data and fits could be the consequence of polymer and CNT polydispersity, if those affect binding (for example, a larger PPO block would promote stronger binding). One indication for polymer polydispersity having an effect on the observed behavior is that the initial decays in both solutions 3 and 4 were often found to be slightly faster than the decay in solution *R*; stronger binding of larger polymers and thereby enrichment of shorter polymers among the free ones is proposed as tentative explanation. These polydispersity effects are, nevertheless, rather moderate; indeed, it seems improbable that a large fraction of polymers would exhibit drastically longer residence times, long enough to be lost in the NMR spectra (see the discussion in the previous subsection).

The residence times in bound states (τ_{bound}) are rather similar for both types of CNT. This observation indicates that the binding mode of F-127 is not necessarily dependent on the substrate (specifically, the curvature of the CNT surface), which is in contrast to what was reported before.[15] The fraction of the bound polymer, p_{bound}, is much larger in the case of SWCNT, which is in line with the much larger available CNT surface (both because of the larger specific surface and because of the larger CNT concentration) in that system. Here, we stress that the surface energy of CNTs seems to be independent of the NT diameter[42] and is close to the value obtained for graphite (~70 mJ m^2).[43,44] The very small degree of carboxylation (see above) is not expected to significantly change this for the MWCNT used here. For SWCNTs manufactured by the same method as the one used here, there exist rather consistent specific surface area (SSA) estimates obtained by Brunauer–Emmett–Teller (BET) analysis of gas adsorption. Using those (SSA = 250 − 300 m^2/g)[45−47] and our estimated concentrations of CNT and F127 (both ca. 3 mg/mL, see Table 2) in the supernatant, we can estimate the nanotube area per F127 molecule as[19]

$$A_{\text{F}-127}(\text{SWCNT}) = \frac{c_{\text{SWCNT}} \times \text{SSA} \times M_{\text{F}-127}}{c_{\text{F}-127} \times p_{\text{bound}} \times N_{\text{A}}} \quad (7)$$

where $M_{\text{F-127}}$ = 12 500 g is the estimated molar mass of the polymer, N_{A} is the Avogadro number, and p_{bound} is as given in Table 3. We obtain $A_{\text{F}-127} \approx 40$ nm^2 which is similar to the value obtained (albeit which a much larger experimental error[19]) for BSA. Here we note that SWCNTs prepared by other methods (e.g., SWNT forest) seem to exhibit other (ca. 1000 m^2/g)[48] SSA values; one might argue that in a SWNT forest all SWNT surface is exposed to gas adsorption and therefore their SSAs are more relevant for a completely dispersed state.

We also observe that the exchange between bound and free states is slower for F-127 than for BSA.[19] For the protein, a partial unfolding of the peptide was assumed for it to be able to bind to the CNT surface. A short lifetime of the partially unfolded state may limit the residence time of BSA. Moreover, it might simply be so that the size of the hydrophobic core of F-127 is larger and/or more hydrophobic than the hydrophobic pocket/patch that has been created on the surface of the unfolded BSA. (As an additional point, we note that certain polymers in SWNT dispersions in organic solvents exhibited site-selective ^{1}H line broadening[49,50] which, most plausibly, seems to be a consequence of fast (in those cases, ≪100 ms) exchange between bound and free states.) On the polymer side, it is the PPO block that determines binding as can be deduced from the finding that PEO chains adsorbed only very weakly at the graphite surface.[51] Therefore, attempts to disperse CNT by PEO of any length results in precipitation. As for Pluronics, the PEO blocks, highly soluble in water, are exploited as sterically stabilizing grafts bound to CNT by the hydrophobic PPO block.

Another kinetic process, relevant for assessing the meaning of our findings, is the exchange of F-127 molecules between free and self-aggregated states that can be studied at concentrations above cmc. Careful analysis of NMR diffusion data has shown that the exchange is fast with residence times within aggregates much below 20 ms,[32] which is in accordance with finding from other kinetic experiments.[52] This, if anything, indicates that the binding of the block copolymer is stronger to CNT than to its self-aggregates. Moreover, at the measured temperature (20 °C) and concentration the F-127 molecules do not form micelles. Pluronics residence times at other surfaces have, to the authors' knowledge and in contrast to some related homopolymers,[53] not yet been determined.

The state of various polymers associated to CNT surfaces has been investigated in numerous molecular dynamics simulations.[22−30] However, studies exploring the behavior of polymers that have strong and specific interactions with CNT (such π–π interactions of polymers with aromatic repeating units) or were performed in vacuum (where hydrophobic interactions are not well manifested) provide less useful comparisons. Irrespective

of those and additional (such as constraints within simulations) limitations, none of the studies seem to report on spontaneous dissociation of the polymer from the CNT surface. Because the typical total time of simulations is in the order or below of 100 ns, the simulation outcomes are in implicit agreement with the much longer residence times we find here. The simulations observe some dynamical modes (such as wrapping-unwrapping) of polymers in continuous contact with the surface and, in some cases, point to a slow surface diffusion that is not in conflict to what has been assumed in the evaluation of our data ($D_{bound} < 10^{-14}$ m^2/s, see above).

CONCLUSIONS

Our TGA and NMR experiments show that, while dispersing CNT in water, Pluronics is found both in the precipitate and the supernatant. This might indicate that the precipitated carbonaceous material, if nanotubes at all, might have different properties than the nanotubes that remain in solution. One such property is stronger binding of Pluronics.

For the nanotubes that remained in solution, we obtained quantitative estimates of the residence times of Pluronics in the bound state, 24 ± 5 ms for SWCNT and of 54 ± 11 ms for MWCNT. Those times, never previously determined, were similar for SWCNT and MWCNT and indicate that the binding of these polymers does not strongly depend on the substrate. However, in comparison to BSA,[19] the exchange between bound and free states was slow, which points to different adsorption modes for those two types of dispersants. Both the obtained residence times and the area per polymer, estimated to be ca. 40 nm^2 in case of SWCNT, provide novel and potentially important limiting or input parameters for simulation studies. In the future, these investigations could be expanded to series of block copolymers to study how the sizes of hydrophobic and hydrophilic parts affect adsorption. In addition, polymers with different assumed binding modes (wrapping versus non-wrapping) could be investigated to be able to see what effect the binding has on residence times.

AUTHOR INFORMATION

Corresponding Author

*E-mail: furo@kth.se.

Notes

The authors declare no competing financial interest.

ACKNOWLEDGMENTS

This study was supported by the Swedish Research Council (VR), the Knut and Alice Wallenberg Foundation, and the Israeli Ministry of Health Grant number 3-00000-6083.

REFERENCES

(1) Haddon, R. C. Special issue: Carbon nanotubes. *Acc. Chem. Res.* **2002**, *35*, 997−1113.

(2) Rueckes, T.; Kim, K.; Joselevich, E.; Tseng, G. Y.; Cheung, C. L.; Lieber, C. M. Carbon nanotube-based nonvolatile random access memory for molecular computing. *Science* **2000**, *289*, 94−97.

(3) Collins, P. G.; Arnold, M. S.; Avouris, P. Engineering carbon nanotubes and nanotube circuits using electrical breakdown. *Science* **2001**, *292*, 706−708.

(4) Jacobs, C. B.; Peairs, M. J.; Venton, B. J. Review: Carbon nanotube based electrochemical sensors for biomolecules. *Anal. Chim. Acta* **2010**, *662*, 105−127.

(5) Bianco, A.; Kostarelos, K.; Prato, M. Applications of carbon nanotubes in drug delivery. *Curr. Opin. Chem. Biol.* **2005**, *9*, 674−679.

(6) Thess, A.; Lee, R.; Nikolaev, P.; Dai, H.; Petit, P.; Robert, J.; Xu, C.; Lee, Y. H.; Kim, S. G.; Rinzler, A. G.; Colbert, D. T.; Scuseria, G. E.; Tomanek, D.; Fischer, J. E.; Smalley, R. E. Crystalline ropes of metallic carbon nanotubes. *Science* **1996**, *273*, 483−487.

(7) Liu, P. Modifications of carbon nanotubes with polymers. *Eur. Polym. J.* **2005**, *41*, 2693−2703.

(8) Bandyopadhyaya, R.; Nativ-Roth, E.; Regev, O.; Yerushalmi-Rozen, R. Stabilization of individual carbon nanotubes in aqueous solutions. *Nano Lett.* **2002**, *2*, 25−28.

(9) Szleifer, I.; Yerushalmi-Rozen, R. Polymers and carbon nanotubes - dimensionality, interactions and nanotechnology. *Polymer* **2005**, *46*, 7803−7818.

(10) Hirsch, A. Functionalization of single-walled carbon nanotubes. *Angew. Chem., Int. Ed.* **2002**, *41*, 1853−1859.

(11) O'Connell, M. J.; Boul, P.; Ericson, L. M.; Huffman, C.; Wang, Y.; Haroz, E.; Kuper, C.; Tour, J.; Ausman, K. D.; Smalley, R. E. Reversible water-solubilization of single-walled carbon nanotubes by polymer wrapping. *Chem. Phys. Lett.* **2001**, *342*, 265−271.

(12) McCarthy, B.; Coleman, J. N.; Czerw, R.; Dalton, A. B.; in het Panhuis, M.; Maiti, A.; Drury, A.; Bernier, P.; Nagy, J. B.; Lahr, B.; Byrne, H. J.; Carroll, D. L.; Blau, W. J. A microscopic and spectroscopic study of interactions between carbon nanotubes and a conjugated polymer. *J. Phys. Chem. B* **2002**, *106*, 2210−2216.

(13) Blanch, A. J.; Lenehan, C. E.; Quinton, J. S. Optimizing surfactant concentrations for dispersion of single-walled carbon nanotubes in aqueous solution. *J. Phys. Chem. B* **2010**, *114*, 9805−9811.

(14) Xin, X.; Xu, G.; Zhao, T.; Zhu, Y.; Shi, X.; Gong, H.; Zhang, Z. Dispersing carbon nanotubes in aqueous solutions by a starlike block copolymer. *J. Phys. Chem. C* **2008**, *112*, 16377−16384.

(15) Shvartzman-Cohen, R.; Florent, M.; Goldfarb, D.; Szleifer, I.; Yerushalmi-Rozen, R. Aggregation and self-assembly of amphiphilic block copolymers in aqueous dispersions of carbon nanotubes. *Langmuir* **2008**, *24*, 4625−4632.

(16) Nativ-Roth, E.; Shvartzman-Cohen, R.; Bounioux, C.; Florent, M.; Zhang, D.; Szleifer, I.; Yerushalmi-Rozen, R. Physical adsorption of block copolymers to SWNT and MWNT: A nonwrapping mechanism. *Macromolecules* **2007**, *40*, 3676−3685.

(17) Monteiro-Riviere, N. A.; Inman, A. O.; Wang, Y. Y.; Nemanich, R. J. Surfactant effects on carbon nanotube interactions with human keratinocytes. *Nanomed. Nanotechnol. Biol. Med.* **2005**, *1*, 293−299.

(18) Moore, V. C.; Strano, M. S.; Haroz, E. H.; Hauge, R. H.; Smalley, R. E. Individually suspended single-walled carbon nanotubes in various surfactants. *Nano Lett.* **2003**, *3*, 1379−1382.

(19) Frise, A. E.; Edri, E.; Furó, I.; Regev, O. Protein dispersant binding on nanotubes studied by NMR self-diffusion and cryo-TEM techniques. *J. Phys. Chem. Lett.* **2010**, *1*, 1414−1419.

(20) Kato, H.; Mizuno, K.; Shimada, M.; Nakamura, A.; Takahashi, K.; Hata, K.; Kinugasa, S. Observations of bound Tween80 surfactant molecules on single-walled carbon nanotubes in an aqueous solution. *Carbon* **2009**, *47*, 3434−3440.

(21) Calvaresi, M.; Dallavalle, M.; Zerbetto, F. Wrapping nanotubes with micelles, hemimicelles, and cylindrical micelles. *Small* **2009**, *5*, 2191−2198.

(22) Yang, M. J.; Koutsos, V.; Zaiser, M. Interactions between polymers and carbon nanotubes: A molecular dynamics study. *J. Phys. Chem. B* **2005**, *109*, 10009−10014.

(23) Zheng, Q. B.; Xue, Q. Z.; Yan, K. O.; Hao, L. Z.; Li, Q.; Gao, X. L. Investigation of molecular interactions between SWNT and polyethylene/polypropylene/polystyrene/polyaniline molecules. *J. Phys. Chem. C* **2007**, *111*, 4628−4635.

(24) Liu, J.; Wang, X. L.; Zhao, L.; Zhang, G.; Lu, Z. Y.; Li, Z. S. The absorption and diffusion of polyethylene chains on the carbon nanotube: The molecular dynamics study. *J. Polym. Sci. B Polym. Phys.* **2008**, *46*, 272−280.

(25) Liu, W.; Yang, C. L.; Zhu, Y. T.; Wang, M. S. Interactions between single-walled carbon nanotubes and polyethylene/polypropylene/polystyrene/poly(phenylacetylene)/poly(p-phen yleneviny-lene) considering repeat unit arrangements and conformations: a

molecular dynamics simulation study. *J. Phys. Chem. C* **2008**, *112*, 1803−1811.
(26) Liu, Y. Z.; Chipot, C.; Shao, X. G.; Cai, W. S. Solubilizing carbon nanotubes through noncovalent functionalization. Insight from the reversible wrapping of alginic acid around a single-walled carbon nanotube. *J. Phys. Chem. B* **2010**, *114*, 5783−5789.
(27) Caddeo, C.; Melis, C.; Colombo, L.; Mattoni, A. Understanding the helical wrapping of poly(3-hexylthiophene) on carbon nanotubes. *J. Phys. Chem. C* **2010**, *114*, 21109−21113.
(28) Tallury, S. S.; Pasquinelli, M. A. Molecular dynamics simulations of flexible polymer chains wrapping single-walled carbon nanotubes. *J. Phys. Chem. B* **2010**, *114*, 4122−4129.
(29) Pang, J. Y.; Xu, G. Y.; Tan, Y. B.; He, F. Water-dispersible carbon nanotubes from a mixture of an ethoxy-modified trisiloxane and pluronic block copolymer F127. *Colloid Polym. Sci.* **2010**, *288*, 1665−1675.
(30) Balamurugan, K.; Gopalakrishnan, R.; Raman, S. S.; Subramanian, V. Exploring the changes in the structure of alpha-helical peptides adsorbed onto a single walled carbon nanotube using classical molecular dynamics simulation. *J. Phys. Chem. B* **2010**, *114*, 14048−14058.
(31) Mills, R. Self-diffusion in normal and heavy water in the range 1−45°. *J. Phys. Chem.* **1973**, *77*, 685−688.
(32) Nilsson, M.; Håkansson, B.; Söderman, O.; Topgaard, D. Influence of polydispersity on the micellization of triblock copolymers investigated by pulsed field gradient nuclear magnetic resonance. *Macromolecules* **2007**, *40*, 8250−8258.
(33) Attal, S.; Thiruvengadathan, R.; Regev, O. Determination of the concentration of single-walled carbon nanotubes in aqueous dispersions using UV-visible absorption spectroscopy. *Anal. Chem.* **2006**, *78*, 8098−8104.
(34) Edri, E.; Regev, O. pH effects on BSA-dispersed carbon nanotubes studied by spectroscopy-enhanced composition evaluation techniques. *Anal. Chem.* **2008**, *80*, 4049−4054.
(35) Josephson, L.; Lewis, J.; Jacobs, P.; Hahn, P. F.; Stark, D. D. The effects of ion oxides on proton relaxivity. *Magn. Reson. Imaging* **1988**, *6*, 647−653.
(36) Hou, P. X.; Bai, S.; Yang, Q. H.; Liu, C.; Cheng, H. M. Multi-step purification of carbon nanotubes. *Carbon* **2002**, *40*, 81−85.
(37) Stejskal, E. O.; Tanner, J. E. Spin diffusion measurements: Spin echoes in the presence of a time-dependent field gradient. *J. Chem. Phys.* **1965**, *42*, 288−292.
(38) Kärger, J. Zur Bestimmung der Diffusion in einem Zweibereichsystem mit Hilfe von gepulsten Feldgradienten. *Ann. Phys. (Berlin)* **1969**, *479*, 1−4.
(39) Kärger, J.; Pfeifer, H.; Henk, W. Principles and application of self-diffusion measurements by nuclear magnetic resonance. *Adv. Magn. Reson.* **1988**, *12*, 1−89.
(40) Schönhoff, M.; Söderman, O. Exchange dynamics of surfactants in adsorption layers investigated by PFG NMR diffusion. *Magn. Reson. Imaging* **1998**, *16*, 683−685.
(41) Schönhoff, M.; Söderman, O. PFG-NMR diffusion as a method to investigate the equilibrium adsorption dynamics of surfactants at the solid/liquid interface. *J. Phys. Chem. B* **1997**, *101*, 8237−8242.
(42) Nuriel, S.; Liu, L.; Barber, A. H.; Wagner, H. D. Direct measurement of multiwall nanotube surface tension. *Chem. Phys. Lett.* **2005**, *404*, 263−266.
(43) Bergin, S. D.; Nicolosi, V.; Streich, P. V.; Giordani, S.; Sun, Z.; Windle, A. H.; Ryan, P.; Niraj, N. P. P; Wang, Z.-T. T.; Carpenter, L.; Blau, W. J.; Boland, J. J.; Hamilton, J. P.; Coleman, J. N. Towards Solutions of Single-Walled Carbon Nanotubes in Common Solvents. *Adv. Mater.* **2008**, *20*, 1876−1881.
(44) Zacharia, R.; Ulbricht, H.; Hertel, T. Interlayer cohesive energy of graphite from thermal desorption of polyaromatic hydrocarbons. *Phys. Rev. B* **2004**, *69*, 155406.
(45) Agnihotri, S. Z., Y. J.; Mota, J. P. B; Ivanov, I.; Kim, P. C. Practical modeling of heterogeneous bundles of single-walled carbon nanotubes for adsorption applications: Estimating the fraction of open-ended nanotubes in samples. *J. Phys. Chem. C* **2007**, *111*, 13747−13755.
(46) Anson, A. J., J.; Parra, J. B.; Sanjuan, M. L.; Benito, A. M.; Maser, W. K.; Martinez, M. T. Porosity, surface area, surface energy, and hydrogen adsorption in nanostructured carbons. *J. Phys. Chem. B* **2004**, *108*, 15820−15826.
(47) Li, F. X. W., Y.; Wang, D. Z.; Wei, F. Characterization of single-wall carbon nanotubes by N-2 adsorption. *Carbon* **2004**, *42*, 2375−2383.
(48) Futaba, D. N.; Hata, K.; Yamada, T.; Hiraoka, T.; Hayamizu, Y.; Kakudate, Y.; Tanaike, O.; Hatori, H.; Yumura, M.; Iijima, S. Shape-engineerable and highly densely packed single-walled carbon nanotubes and their application as super-capacitor electrodes. *Nat. Mater.* **2006**, *5*, 987−994.
(49) Star, A.; Stoddart, J. F.; Steuerman, D.; Diehl, M.; Boukai, A.; Wong, E. W.; Yang, X.; Chung, S.-W.; Choi, H.; Heath, J. R. Preparation and properties of polymer-wrapped single-walled carbon nanotubes. *Angew. Chem., Int. Ed.* **2001**, *40*, 1721−1725.
(50) Chen, J.; Liu, H. Y.; Weimer, W. A.; Halls, M. D.; Waldeck, D. H.; Walker, G. C. Noncovalent engineering of carbon nanotube surfaces by rigid, functional conjugated polymers. *J. Am. Chem. Soc.* **2002**, *124*, 9034−9035.
(51) Holland, N. B.; Xu, Z.; Vacheethasanee, K.; Marchant, R. E. Structure of poly(ethylene oxide) surfactant polymers at air-water and solid-water interfaces. *Macromolecules* **2001**, *34*, 6424−6430.
(52) Zana, R.; Marques, C.; Johner, A. Dynamics of micelles of the triblock copolymers poly(ethylene oxide)-poly(propylene oxide)-poly(ethylene oxide) in aqueous solution. *Adv. Colloid Interface Sci.* **2006**, *123*, 345−351.
(53) Boissier, C.; Lofroth, J. E.; Nyden, M. Water-based latex dispersions. 3. Exchange dynamics of nonionic surfactants and poly(ethylene glycol) on colloidal particles with different interfacial properties. *J. Phys. Chem. B* **2003**, *107*, 7064−7069.